

## Tunable gold-chitosan nanocomposites by local field engineering

Ana Cazacu, Lavinia Curecheriu, Alexandra Neagu, Leontin Padurariu, Adrian Cernescu, Isabelle Lisiecki, and Liliana Mitoseriu

Citation: [Applied Physics Letters](#) **102**, 222903 (2013); doi: 10.1063/1.4809673

View online: <http://dx.doi.org/10.1063/1.4809673>

View Table of Contents: <http://scitation.aip.org/content/aip/journal/apl/102/22?ver=pdfcov>

Published by the [AIP Publishing](#)

---



# FREE Multiphysics Simulation e-Magazine

DOWNLOAD TODAY >>

 COMSOL

## Tunable gold-chitosan nanocomposites by local field engineering

Ana Cazacu,<sup>1,2</sup> Lavinia Curecheriu,<sup>1,a)</sup> Alexandra Neagu,<sup>1</sup> Leontin Padurariu,<sup>1</sup>  
 Adrian Cernescu,<sup>3</sup> Isabelle Lisiecki,<sup>4</sup> and Liliana Mitoseriu<sup>1,b)</sup>

<sup>1</sup>Department of Physics, Al. I. Cuza University, Bd. Carol I, No. 11, Iasi 700506, Romania

<sup>2</sup>Department of Chemical and Processing Engineering, University of Genoa, via Balbi, 5, 16126 Genoa, Italy

<sup>3</sup>Max Planck Institute of Quantum Optics, Am Coulombwall 1, D-85741 Garching, Germany

<sup>4</sup>Laboratoire des Matériaux Mésooscopiques et Nanométriques, UMR CNRS 7070,  
 Université Pierre et M. Curie, Bât. F, 4 Place Jussieu, 75005 Paris, France

(Received 21 February 2013; accepted 19 May 2013; published online 5 June 2013)

A method to control the permittivity and tunability in composite materials formed by conductive nanoparticles embedded in a flexible nonlinear dielectric matrix is proposed. The local field distributions in composite structures were determined and the field-induced permittivity was estimated for different volume fraction of conductive particles. The predicted tunability behavior agrees well with the observed trends obtained for gold nanoparticles embedded in chitosan matrix. The paper demonstrates the concept of engineered local fields in nanocomposites by using metallic nanoparticles as fillers in polymer matrix for tailoring the permittivity and tunability values. © 2013 AIP Publishing LLC. [<http://dx.doi.org/10.1063/1.4809673>]

The nonlinear properties of dielectric materials are of great interest nowadays, due to the potential applications in miniaturized microwave devices and for integration in micro-electronic circuits.<sup>1,2</sup> Promising results were reported especially in film structures of the most studied solid solutions of (Ba,Sr)TiO<sub>3</sub> (BST)<sup>3</sup> and (Pb,Sr)TiO<sub>3</sub> (PST).<sup>4</sup> Usually, high tunability  $n(E) = \varepsilon(0)/\varepsilon(E)$  is obtained in ferroelectric structures and is accompanied by large permittivity, which is contradictory with the application requirements needing for moderate permittivity ( $\varepsilon$  below 1000), large tunability, and low dielectric losses (below 3%).<sup>5</sup> Therefore, a higher tunability together with a reduction of dielectric constant is strongly desired. To increase the tunability, the approach of dispersing homogeneous conductive particles in ferroelectric matrix (Ag-BST<sup>6</sup> and Ag-PST<sup>7</sup>) was developed, but the method leads to high dielectric constant, due to the formation of microcapacitors. In order to preserve high tunability but to reduce permittivity keeping low losses, other methods were proposed: (i) doping ferroelectrics with different ions (such as La<sup>3+</sup>, Co<sup>3+</sup>, Mg<sup>2+</sup>, Mn<sup>2+</sup>, In<sup>3+</sup>)<sup>8</sup> to shift the ferroelectric-paraelectric transition towards room temperature and drive the permittivity to requested values (usually in the paraelectric state) and (ii) forming composites of BaTiO<sub>3</sub>-based solid solutions with low-permittivity non-ferroelectrics as MgO, MgTiO<sub>3</sub>, or Al<sub>2</sub>O<sub>3</sub>.<sup>9–11</sup> Recently, we proposed the concept of tailoring the nonlinear properties of ferroelectric and dielectric structures by local field engineering.<sup>12</sup> It was demonstrated that a composite material formed by linear dielectric inclusions into a ferroelectric matrix can satisfy the high tunability and low permittivity requirements, due to the local field on the ferroelectric component which is tuned by the linear dielectric component.<sup>12</sup> The calculations showed that, for any nonlinear dielectric matrix, the local field can be engineered by using different types of inclusions (dielectric, conductive, air pores, etc.) and such composite will present a tailored effective tunability. This paper is focused on testing

this concept for the case of composite materials formed by conductive nanoparticles embedded in a flexible nonlinear dielectric matrix.

The estimation of permittivity vs. field dependence in a composite material should be computed by considering the local field inhomogeneity. In order to solve this problem, a virtual 2D (1 cm × 1 cm) model of planar sample was considered. The local electric potential is described by the Poisson's equation:  $\nabla \cdot (\varepsilon(x, y) \nabla V) = 0$ , in which a constant permittivity for inclusions and a field dependent local permittivity for the dielectric is considered. The largely accepted formula for the permittivity vs. field variation both for ferroelectric or relaxors in their paraelectric state and for polar dielectrics at high fields is given by the Johnson approach<sup>13</sup>

$$\varepsilon(x, y) = \varepsilon_r(0) / (1 + \beta \cdot \varepsilon_r(0)^3 E_{local}^3)^{1/3}, \quad (1)$$

in which  $\varepsilon_r(0)$  is the permittivity at zero field,  $E$  is the external applied field, and  $\beta$  is a coefficient describing the ferroelectric nonlinearity.

The Poisson's equation is solved by the Finite Element Method (FEM) taking into account the Dirichlet/Neumann boundary conditions (Figs. 1(a) and 1(c)) and considering the dependence of the local permittivity on the local field for different applied voltages. The effective permittivity can be derived from the total energy  $W_t = (\varepsilon_{eff} \cdot E_{app}^2 / 2) \cdot V_t$  (where  $E_{app}$  is the applied field and  $V_t$  is the total volume of the virtual samples) which is computed as a sum of the local energies  $W_t = \iiint (\varepsilon \cdot \nabla V^2) dx dy dz$ . More details of simulation procedure were given elsewhere.<sup>12,14</sup>

Different kinds of virtual microstructures with different compositions have been numerically generated and the local electric field was computed by FEM. The numerical values in simulation were chosen in such way that the permittivity of the pure nonlinear phase is 40 at zero field and almost half at 500 kV/cm applied field. This dependence describes a non-ferroelectric polar system whose tunability (the ratio between the zero field permittivity and the field-induced

<sup>a)</sup>E-mail: [lavinia\\_curecheriu@stoner.phys.uaic.ro](mailto:lavinia_curecheriu@stoner.phys.uaic.ro)

<sup>b)</sup>E-mail: [lmstr@uaic.ro](mailto:lmstr@uaic.ro)

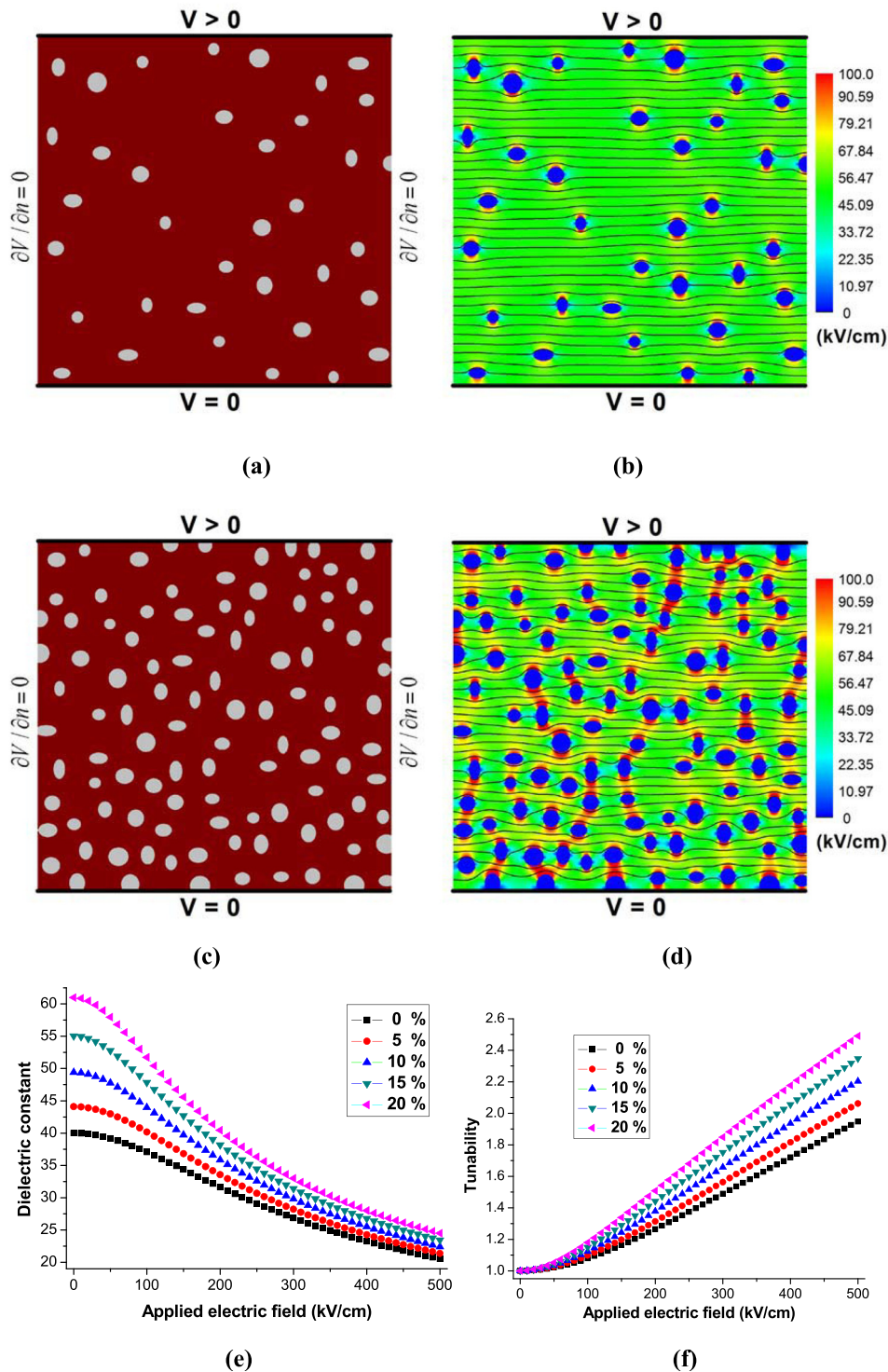


FIG. 1. Simulated composite microstructures with different volume filling factors of the conductive particles (grey color): (a)  $f = 5\%$  and (c)  $f = 15\%$  in the nonlinear dielectric matrix (brown); and (b), (d) the corresponding local field maps. The intensity of the local electric field is represented in color scale, and the field direction is perpendicular on the isopotential lines (black lines). Note that isopotential lines are agglomerated in high field regions; (e), (d) computed permittivity and tunability vs. the applied voltage for composite with different volume filling factors of conductive nanoparticles.

permittivity) becomes significant at much higher fields than typically reported for ferroelectric or relaxor tunable materials (of  $\sim 30$  kV/cm).<sup>15,16</sup> The permittivity of the conductive inclusions was chosen to be  $10^5$ , i.e., infinite by comparison to the permittivity of the matrix. Such a high value is justified by the existence of free charges in conductors, which redistribute in the presence of an electric field in such a way to result an infinite polarization. By comparison, dielectrics contain bounded charges, which create a finite polarization, and hence they have a finite permittivity.

Figs. 1(a) and 1(c) show a simulated composite microstructure (similar to a 0–3 connectivity) formed by a

homogeneous dispersion of conductive nanoparticles (gray inclusions) into a nonlinear dielectric matrix (brown). For the generated microstructures, the local field patterns were calculated and the results were presented in Figs. 1(b) and 1(d). As it can be observed, by increasing the number of conductive particles, the fields inside the sample become more inhomogeneous and enhanced. The high field is predominantly located in the nonlinear dielectric regions nearby the metal-dielectric interfaces, perpendicular on the applied field direction. The electric field inside each conductive inclusion is null. The regions subjected to very high fields increase with increasing the addition of conductive inclusions

(Fig. 1(d)), which will cause an enhanced tunability of the overall system. Therefore, the presence of metallic inclusions below the percolation limit is expected to produce an increase of both the effective permittivity and tunability, by comparison with the pure non-linear dielectric values. Further, the effective permittivity under the external field  $\varepsilon_{eff}(E_{app})$  dependences was computed for different conductive particles contents and the results are shown in Fig. 1(e). Both the effective permittivity and tunability are larger when the conductive particles additions are higher. The tunability increase can be correlated with the increase of the maximum local field inside the composite, as observed in the local field distributions (Figs. 1(b) and 1(d)). Therefore, different levels of tunability and increased permittivity can be tailored by engineering the conductive addition in the nonlinear matrix.

To validate the proposed approach, the nonlinear dielectric character of polymer-metallic nanoparticles (NPs) composites was tested. The use of metallic nanofillers in polymer-based composites has attracted interest due to possible application in low cost flexible electronics. Metal NPs as Cu, Ni, Pd, and their alloys are basic components for circuit interconnectors, electrodes in capacitors, resistors and diodes, mechanical structures, and optical parts in microelectromechanical systems (MEMS). An innovative potential use of metallic NPs in organic matrices emerged from the need to increase permittivity in polymer-based structures for high volume capacitance in microelectronics and energy storage applications. The dielectric non-linearity usually accompanies ferroelectric/relaxor state and it has still not been accomplished in flexible materials at reasonable fields. Therefore, the predictions of the present FEM analysis which showed the possibility of increasing tunability of a polar dielectric by adding metallic fillers were checked in thick films of gold (Au) NPs embedded in chitosan (Chi) matrix. Chitosan is a cheap naturally derived polymer with unique chemical properties. This polymer has the ability to integrate in its structure assembly of biomolecules, cells, and inorganic nanoparticles. Its potential use in integrated devices and biological functionalization MEMS was recently reported.<sup>17</sup> The electrical properties of noble metal NPs-Chi nanocomposites became interesting for potential applications as biosensors and electrolytes for fuel cells;<sup>18</sup> however, high-field electrical characteristics and their nonlinear dielectric character were never tested or exploited.

Au NPs in different concentrations dispersed in Chi films were prepared by dry phase inversion from an aqueous solution of Chi obtained by mixing 1% Chi (practical grade type, 263,836 g/mol average molecular weight) previously dissolved in a 1% (v/v) acetic acid solution with different quantities of 1 mM HAuCl<sub>4</sub>. All the materials used were purchased from Sigma Aldrich. The solutions were cast into Teflon molds and left to dry in a thermostat chamber at 50 °C for 24 h (according to the dry phase inversion method of thin film preparation).<sup>19</sup> The samples are denoted in the following as 0 Chi (40 ml Chi); 2 Chi (38 ml Chi + 2 ml HAuCl<sub>4</sub>, and  $f=0.4\%$ ), 6 Chi (34 ml Chi + 6 ml HAuCl<sub>4</sub>, and  $f=1.5\%$ ), 8 Chi (32 ml Chi + 8 ml HAuCl<sub>4</sub>, and  $f=2\%$ ), and 10 Chi (30 ml Chi + 10 ml HAuCl<sub>4</sub>, and  $f=2.5\%$ ), taking into account the volume fraction of the employed HAuCl<sub>4</sub>.

The samples morphology and AuNP dispersion into the Chi films were determined by scattering scanning near-field optical microscopy (s-SNOM), which employs a commercial scattering near-field microscope (NeaSNOM, Neaspec.com) equipped with a standard metalized tip. For electric measurements, silver electrodes were applied by RF sputtering on Chi films. The dielectric constant and dissipation factor were measured at room temperature in the frequency range (1–10<sup>6</sup>) Hz by using an Impedance/Gain-Phase analyzer SOLARTRON 1260A. The tunability  $\varepsilon(E)$  characteristics were determined using a circuit fed by a high dc voltage from a function dc-generator coupled with a TREK 30/20A-H-CE amplifier<sup>20</sup> superimposed on a small ac testing voltage (1 V) with a frequency of  $3 \times 10^4$  Hz.

The topography and near-field optical images of Chi film as well as Au-Chi films were recorded (Fig. 2). With an average size of about 15 nm, the Au NPs can be easily distinguished from larger local impurities, especially due to their low optical contrast surrounded by a bright ring. The metalized tip of s-SNOM, under external infrared illumination, acts as a light-concentrating antenna such that the sample is probed with a nanofocused light field. Detection of the back-scattered light reveals local optical information with maximum resolution imposed by the AFM tip size (around 20 nm) and independent of the laser wavelength.<sup>21,22</sup> The observable contrasts can be derived from the complex dielectric function of the sample material<sup>23</sup> and include both the absolute efficiency and the phase of the scattering.

It is known that the near-field optical nanoparticle contrast depends on both the electrical properties of the particles and their size.<sup>24</sup> Quite interesting, in the optical images, the Au NPs exhibit bright rings, as the backscattered signal of the Chi is enhanced in their close vicinity (20–40 nm). As recently reported,<sup>24</sup> this observation can be associated with a locally increased concentration of the collective free-electron

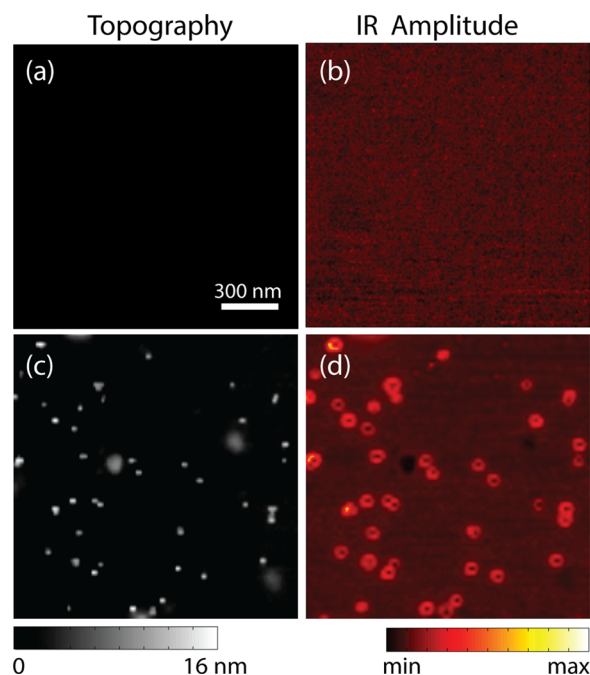


FIG. 2. S-SNOM images ( $1.5 \times 1.5 \mu\text{m}^2$ ) of pure Chi and Au-Chi films. In the left side is presented the topography, and in the right side the backscattered IR amplitude recorded at 3rd order demodulation frequency.

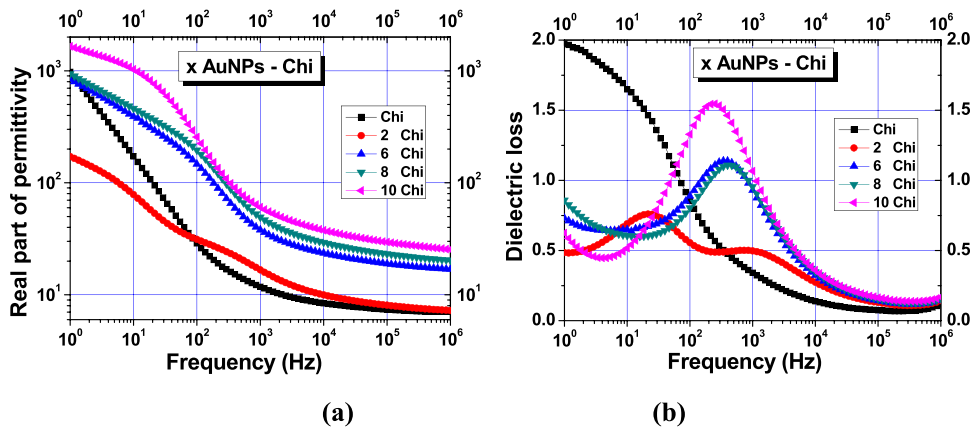


FIG. 3. Frequency dependence of the dielectric constant (a) and tangent loss (b) for Au-Chi nanocomposites with different compositions.

oscillations (plasmons) and therefore a higher conductivity of the Chi matrix close to the Au NPs, which clearly is related to the strong increase of the local field at the metallic NPs-Chi interface, as predicted by the FEM calculations.

Figures 3(a) and 3(b) show the frequency dependence of the dielectric constant and losses for Au-Chi films with different Au NPs content. Interface phenomena and electrode effects cause an increase of the low-frequency permittivity and losses and only at high frequencies above 10 kHz, the composite thick films have a predominant dielectric character. In high frequency range, the dielectric loss  $\tan \delta$  is about 10%–23% and the permittivity monotonously increases with Au addition between 8 and 28 (Fig. 3(a)), due to the fact that metallic NPs act as internal conductive electrodes inside the sample. When the content of Au NPs is higher, the number of such microcapacitors and the distance between them (capacitor thickness) increase and the effective dielectric constant increases, as predicted by the FEM calculations.<sup>25</sup> For all the compositions, the permittivity decreases with frequency increasing and a complex dispersion behavior characterized by distinct relaxation phenomena (multiple maxima of losses) in the range of 1–100 Hz and in kHz range, respectively, is noticed. The peak around  $10^3$  Hz (Fig. 3(b)) is originated from the  $\alpha$ -relaxation of chitosan membranes<sup>26</sup> and shifts towards low frequency with Au NPs addition. A detailed analysis of the dielectric relaxation phenomena is beyond the scope of the present paper, but it is worth to notice that such a trend is typically reported in nanocomposite films<sup>7</sup> and is explained by considering multiple polarization mechanisms which contribute to the dielectric behavior.<sup>27</sup> The interfaces between dissimilar phases,

particularly in nanostructured materials, are sites for local uncompensated charges, which move under alternative fields and give rise to dipolar contributions (space charge effects) to the total polarization. The space charge polarization acts as extrinsic phenomena usually at low frequency and is responsible for relative high values of low frequency dielectric losses. Therefore, the high field properties were checked at a testing frequency of  $3 \times 10^4$  Hz.

The permittivity vs. field  $\varepsilon(E)$  dependence (dc-tunability) determined at room temperature at increasing/decreasing dc-field cycle are shown in Fig. 4(a). A permittivity nonlinearity is observed for all the compositions and in particular for high Au NPs additions, with a tendency towards saturation (but not yet obtained, even at high fields of  $\sim 900$  kV/cm) and with a small hysteresis. After the first increasing/decreasing voltage cycles, the non-linear field-dependence  $\varepsilon(E)$  tends to stabilize to a non-hysteretic behavior and the tunability properties are well reproducible.

For all the applied dc fields, the tunability  $n(E)$  increases with Au NPs addition and reaches the value of  $\sim 2.3$  for the maximum addition (sample 10 Chi) by comparison with values of  $\sim 2$  in pure Chi films (at the maximum applied field). Qualitatively, the field dependence of tunability in Fig. 4(b) is similar to the one predicted by FEM calculations in Fig. 1(f). If for the pure Chi films the nonlinear dielectric response  $\varepsilon(E)$  is caused by the polar region reorientations under the high fields, the increase of tunability with Au NPs addition increasing is induced by the local field distributions. More specific, the polar character of chitosan responsible for its high-field non-linear dielectric response is enhanced by increasing the local fields produced by the presence of

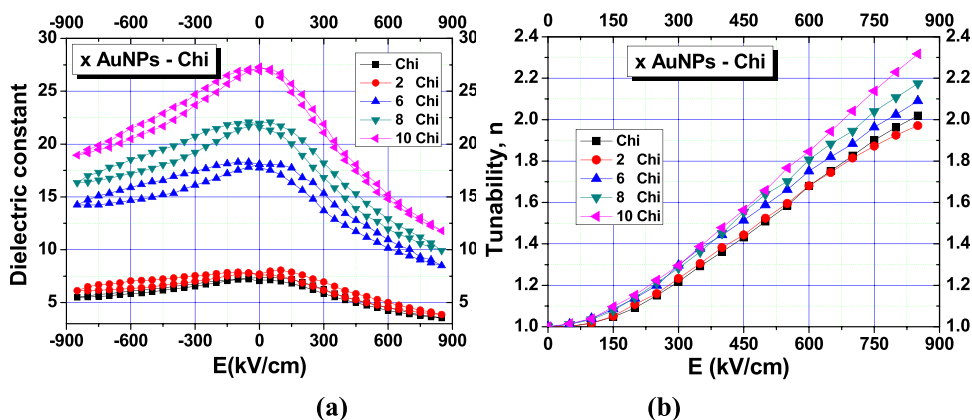


FIG. 4. (a) Dielectric constant vs. applied dc field; (b) field dependent tunability for Au-Chi nanocomposite films with different Au NPs additions.

metallic nanoparticles in Au NPs-Chi composites. As FEM calculations predicted, the local field inhomogeneity created by the addition of metallic nanoparticles helps in increasing both permittivity and tunability values.

To summarize, the present paper shows a proof of concept for modifying the permittivity and tunability values in nanocomposites by local field engineering, using metallic NPs as fillers in polymer matrix. Even though the tunability increase is still low and needs high field values, it is important to conclude that local fields can be engineered to some extent in well-defined microstructures and this effect can be exploited to tailor a new class of flexible tunable materials.

This work is dedicated to the memory of our colleague, Professor Viorel Melnig. We thank F. Keilmann and S. Amarie for discussions. The financial support of the POSDRU/89/1.5/S/63663 (Ana Cazacu) and Romanian CNCS-UEFISCDI Project Nos. PN-II-ID-PCE-2011-3-0745 and PN –II-RU-TE-2012-3-0150 is highly acknowledged.

- <sup>1</sup>J. Im, O. Auciello, P. K. Baumann, S. K. Streiffer, D. Y. Kaufman, and A. R. Krauss, *Appl. Phys. Lett.* **76**, 625 (2000).
- <sup>2</sup>C. L. Canedy, H. Li, S. P. Alpay, L. S. Riba, A. L. Roytburd, and R. Ramesh, *Appl. Phys. Lett.* **77**, 1695 (2000).
- <sup>3</sup>S. J. Lee, S. E. Moon, H. C. Ryu, M. H. Kwak, Y. T. Kim, and S. K. Han, *Appl. Phys. Lett.* **82**, 2133, (2003).
- <sup>4</sup>W. Kleemann, J. Dec, R. P. Wang, and M. Itoh, *Phys. Rev. B* **67**, 092107 (2003).
- <sup>5</sup>A. K. Tagantsev, V. O. Sherman, K. F. Astafiev, J. Venkatesh, and N. Setter, *J. Electroceram.* **11**, 5 (2003).
- <sup>6</sup>J. Huang, Y. Cao, and M. Hong, *Appl. Phys. Lett.* **92**, 022911 (2008).
- <sup>7</sup>Z. Wang, T. Hu, X. Li, G. Han, W. Weng, N. Ma, and P. Du, *Appl. Phys. Lett.* **100**, 132909 (2012).

- <sup>8</sup>M. W. Cole, P. C. Joshi, and M. H. Ervin, *J. Appl. Phys.* **89**, 6336–6340 (2001).
- <sup>9</sup>R. H. Liang, X. L. Dong, Y. Chen, F. Cao, and Y. L. Wang, *Jpn. J. Appl. Phys., Part 1* **43**, 201–204 (2004).
- <sup>10</sup>U.-C. Chung, C. Elissalde, M. Maglione, C. Estournes, M. Pate, and J. P. Ganne, *Appl. Phys. Lett.* **92**, 042902 (2008).
- <sup>11</sup>M. W. Cole, P. C. Joshi, M. H. Ervin, M. C. Wood, and R. L. Pfeffer, *Thin Solid Films* **374**, 34 (2000).
- <sup>12</sup>L. Padurariu, L. Curecheriu, C. Galassi, and L. Mitoseriu, *Appl. Phys. Lett.* **100**, 252905 (2012).
- <sup>13</sup>K. Johnson, *J. Appl. Phys.* **33**, 2826 (1962).
- <sup>14</sup>L. Padurariu, L. Curecheriu, V. Buscaglia, and L. Mitoseriu, *Phys. Rev. B* **85**, 224111 (2012).
- <sup>15</sup>Z. Yu, C. Ang, R. Guo, and A. S. Bhalla, *Appl. Phys. Lett.* **81**(7), 1285–1287 (2002).
- <sup>16</sup>A. Tkach, P. M. Vilarinho, and A. Kholkin, *J. Appl. Phys.* **101**, 084110 (2007).
- <sup>17</sup>S. T. Koev, P. H. Dykstra, X. Luo, G. W. Rubloff, W. E. Bentley, G. F. Payne, and R. Ghodssi, *Lab Chip* **10**, 3026–3042 (2010).
- <sup>18</sup>E. Prokhorov, J. G. Luna-Bárceñas, J. B. Gonzalez-Campos, and I. C. Sanchez, *Mol. Cryst. Liq. Cryst.* **536**, 24–32 (2011).
- <sup>19</sup>A. Garlea, V. Melnig, and M. I. Popa, *J. Mater. Sci.: Mater. Med.* **21**(4), 1211–1223 (2010).
- <sup>20</sup>L. P. Curecheriu, Ph.D. dissertation, University Al. I. Cuza, 2009.
- <sup>21</sup>B. Knoll and F. Keilmann, *Nature* **399**, 134–137 (1999).
- <sup>22</sup>M. Brehm, T. Taubner, R. Hillenbrand, and F. Keilmann, *Nano Lett.* **6**, 1307–1310 (2006).
- <sup>23</sup>A. Cvitkovic, N. Ocelic, and R. Hillenbrand, *Nano Lett.* **7**, 3177–3181 (2007).
- <sup>24</sup>J. M. Stiegler, R. Tena-Zaera, O. Idigoras, A. Chuvilin, and R. Hillenbrand, *Nat. Commun.* **3**, 1131 (2012).
- <sup>25</sup>S. Georgea and M. T. Sebastian, *Compos. Sci. Technol.* **68**, 2461–2467 (2008).
- <sup>26</sup>J. B. Gonzalez-Campos, E. Prokhorov, G. Luna-Bárceñas, A. Fonseca-García, and I. C. Sanchez, *J. Polym. Sci., Part B: Polym. Phys.* **47**, 2259–2271 (2009).
- <sup>27</sup>M. Chi-Mel, Z. Lide, and W. Guozhong, *Nanostruct. Mater.* **6**, 823–826 (1995).